Influence of the t_{33}-stress on the 3-D stress state around corner cracks in an elastic plate

V.F. González-Albuixech [a], E. Giner [a,*], J. Fernández-Sáez [b], A. Fernández-Canteli [c]

[a] *Centro de Investigación de Tecnología de Vehículos - CITV, Depto. de Ingeniería Mecánica y de Materiales, Universidad Politécnica de Valencia, Camino de Vera, 46022 Valencia, Spain.*

[b] *Dept. of Continuum Mechanics and Structural Analysis, University Carlos III of Madrid, Av. Universidad, 30, 28911 Leganés, Madrid, Spain.*

[c] *Dept. of Construction and Manufacturing Engineering, E.P.S. de Ingeniería de Gijón, University of Oviedo, Campus de Viesques, 33203 Gijón, Spain.*

Abstract

When an analysis of the 3-D crack behavior in LEFM is performed, usually only the first term of the Williams series expansion, which corresponds to the $r^{-\frac{1}{2}}$ singularity, is taken into account. However, it is well known that t_{ij} stresses (second order terms) have still influence. Even when t_{ij} stress terms are introduced, the only term usually taken into account corresponds to the t_{11} factor, generally called T-stress. If a correct 3-D description has to be done, the t_{33} term has also to be considered. In this work, the relevance of the t_{33} stress term in the analysis of a mode I corner crack is shown in contrast to other approaches that use certain *ad hoc* parameters, such as the so called T_z-constraint factor proposed by Guo and co-workers. The analysis is carried out for elliptical corner cracks with different aspect ratios, showing that the introduction of the t_{33} description avoids the approximations inherent to the T_z approach.

Key words: t_{33}-stress; T_z constraint factor; T-stress; quarter-elliptical corner crack; finite element analysis.

---

* Corresponding author. Tel.: +34-96-3877621; fax: +34-96-3877629.
Email address: `eginerm@mcm.upv.es` (E. Giner).

Preprint submitted to Engng Fract Mech *26 October 2010*

NOMENCLATURE

a	Crack length (minor axis of the quarter-elliptical crack)
A_i, B_{ij}	Fitted parameters of the T_z distribution
c	Crack length (major axis of the quarter-elliptical crack)
E	Young's modulus
$f_{ij}(\theta)$	Angular function related to the singular term of σ_{ij}
$f_{33,T_z}(\theta)$	Angular function generated with $T_{z(\theta=0)}$
h	Specimen half height
J	Pointwise value of the J-integral at a given location of the crack front
K_{I}	Stress intensity factor under mode-I loading
r	In-plane radial distance to the crack front (polar coordinate)
t	Specimen thickness
t_{11}	Constant stress in the x_1-direction (second order term of σ_{11})
t_{33}	Constant stress in the x_3-direction (second order term of σ_{33})
t_{ij}	Generic notation for the constant stress components
$T \equiv t_{11}$	T-stress (constant stress in the x_1-direction)
T_z	Out-of-plane constraint factor
$T_{z(\theta=0)}$	Out-of-plane constraint factor estimated at $\theta = 0$
u_3	Out-of-plane displacement
V	Integration volume for J_{vol}
w	Specimen width
W	Strain energy density
δ_{ij}	Kronecker's delta
ε_{33}	Out-of-plane normal strain
φ	Parametric angle used to define the crack front location
ν	Poisson's ratio
σ	Uniform applied stress
σ_{11}, σ_{22}	In-plane components of σ_{ij}
σ_{33}	Out-of-plane component of σ_{ij}
θ	In-plane orientation angle (polar coordinate)
$O(r^{1/2})$	Generic higher order terms in Williams expansion

1 INTRODUCTION

Three-dimensional (3-D) corner cracks typically occur at stress concentrations, such as the surfaces of bolted or riveted joints, the edges of fastener holes in lugs, stiffeners and other aircraft components and mechanical structures [1–3]. The growth of such cracks usually causes premature failure and therefore, much attention has long been paid to the fatigue crack propagation analysis and damage tolerance design [4,5]. In these situations, the triaxial stress field near the crack front has an important role in a fracture mechanics framework [6–9]. Basically, the existing triaxial constraints are the in-plane and out-of-plane constraints and both are related to the geometry and loading configuration of the cracked structure.

The in-plane constraint is essentially dominated by the dimensions in the normal plane to the crack front and the out-of-plane constraint is mainly determined by the dimensions parallel to the crack front (i.e. in the thickness direction), together with the boundary conditions. Constraints have an important effect on the observed toughness of the structural components in 3-D, as is shown in [10] through a finite element study, analyses of round bars [11] or in statistical studies on the effect of constraints on standardized specimens [9]. Consequently, it is important to gain a better understanding of the stress field around the crack front including 3-D constraint components.

The crack stress state is usually described using the local reference coordinate system shown in Fig. 1, where 1 is the direction normal to the crack front contained in the crack plane, direction 2 is normal to the crack surface and direction 3 is tangent to the crack front.

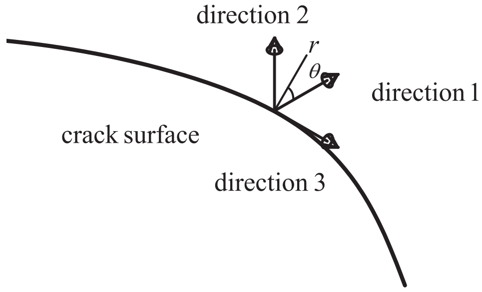

Fig. 1. Local reference coordinate system for a crack front.

In accordance with this reference system, the Williams series expansion [12–14], generalized to 3-D, is given by

$$\sigma_{ij} = \frac{K}{\sqrt{2\pi r}} f_{ij}(\theta) + t_{ij} + O(r^{1/2}) \tag{1}$$

It is observed that the second terms do not depend on r. The second term in direction 1, t_{11}, is usually known as T-stress. In addition, the t_{33} component is also present in the tangential direction. Numerically, the t_{11} term (T-stress) can be obtained using the interaction integral proposed in [13] and the t_{33} stress term can be inferred from t_{11} and the elastic fields, as detailed in the next section. These terms affect the triaxiality in the near tip stress fields and are directly related to the in-plane and out-of-plane constraints: t_{11} is related to the in-plane constraint and t_{33} is related to the out-of-plane constraint. The t_{ij}-stress terms, together with the stress intensity factor (SIF), can provide a set of practical parameters for the characterization of near crack tips fields, nominally K-t_{ij}, see e.g. [14–16]. Moreover some works [17–19] provide comprehensive tables containing approximated t_{ij} values for specifical crack configurations.

Another widely extended approach used for characterizing the out-of-plane constraint is the T_z factor, proposed by Guo [20–22]. T_z is a factor which is used in the definition of the stress state field σ_{33} to reflect the out-of-plane constraint influence. In this case, the set of characterizing parameters is K-T-T_z [23]. Some studies on the application of the T_z factor for the quarter-elliptical or semi-elliptical crack have been carried out [24,25]. In these works, the T_z approach does not consider the existence of t_{33} and T_z is estimated performing a least square approximation from numerical results.

If a proper study of the crack behavior is to be done, the nonzero t_{ij} terms have to be included in the stress state description near the crack front. In this work, t_{33} is considered as an alternative parameter to T_z, showing its influence on the triaxiality. By means of numerical examples, it is shown that it has to be considered in the stress field description to achieve accurate approximations.

The outline of the paper is as follows. In Section 2, a brief review of the stress state around a 3-D crack front, including second order terms, is presented. Then, a short description of the T_z approach [24] is given in Section 3. The main results of the work are presented in Section 4, where several quarter-elliptical corner crack analyses are performed using finite elements. The results considering the t_{33}-stress and the T_z parameter are compared, showing that the use of the components of the t_{ij} tensor provides a better description of the stress state. Finally, some conclusions are summarized in Section 5.

2 STRESS STATE AROUND A 3-D CRACK FRONT

Some works on the analysis of the stress state for 3-D cracks in LEFM can be found in the literature. To name a few, Hartranft and Sih [26] introduced a series expansion for an infinite domain using eigenfunction methods on cylindrical local coordinates. In [27], Sih introduced the thickness influence on the crack stress field as a stress state change from a plane strain to a plane stress state. Benthem [28] took into consideration the effect of the free boundaries on the stress state for a 3-D crack front orthogonal to the surface, whereas in [29], Pook considered the effect of the angle between the crack front and the free boundary. Kwon and Sun [30] discussed the divergence of the crack 3-D stress state from the corresponding plane strain state, which is commonly accepted as hypothesis. These and other works provide insights into the 3-D crack problem, although, unfortunately, it is commonly accepted that the 3-D crack problem remains unsolved in a general way.

The main practical developments on this field still rely on concepts and results obtained from 2-D solutions, as the plane strain and plane stress state assumptions. However, nowadays it is accepted that the plane strain and plane stress concepts cannot be directly generalized to 3-D crack problems [27]. Moreover, under LEFM assumptions, the so-called corner singularity exists at the intersection of the crack front with the free surface, whose order depends of the Poisson's ratio [28]. As the effect of this singularity is assumed to be limited to a short ranged distance [29–31], we will accept that it happens sufficiently far from the region where the fields are studied and it is not taken into consideration in this work. Therefore, we will use the description of the singular stress fields in the vicinity of the crack front in accordance to the Williams series expansion. As mentioned in the introduction, second order terms in this expansion cannot be, in general, neglected in a region close to the crack front. Although the in-plane T-stress is usually considered in the 2-D and 3-D studies, the out-of-plane component t_{33} also plays an important role in the constraint effects [14,15,17] and it has to be considered, as proposed in this work.

Sufficiently close to the crack front to neglect higher order terms and ignoring the effects of corner singularities, the expressions for the normal components of the near tip stress fields corresponding to symmetric (mode-I) loading are:

$$\begin{aligned}
\sigma_{11}(r,\theta) &= \frac{K_{\mathrm{I}}}{\sqrt{2\pi r}}\cos\frac{\theta}{2}\left(1-\sin\frac{\theta}{2}\sin\frac{3\theta}{2}\right)+t_{11}\\
\sigma_{22}(r,\theta) &= \frac{K_{\mathrm{I}}}{\sqrt{2\pi r}}\cos\frac{\theta}{2}\left(1+\sin\frac{\theta}{2}\sin\frac{3\theta}{2}\right)\\
\sigma_{33}(r,\theta) &= \frac{K_{\mathrm{I}}}{\sqrt{2\pi r}}2\nu\cos\frac{\theta}{2}+t_{33}
\end{aligned} \tag{2}$$

as given for example in [13]. Eqs. (2) are expressed in the local reference coordinate system of Fig. 1. It is well known that K_{I} varies along the local coordinate 3, and so do t_{11}, t_{33} as shown in [15,17–19]. Only t_{11} and t_{33} terms appear in Eq. (2), being the other t_{ij} components zero due to symmetry considerations and the traction free condition of crack faces.

2.1 Out-of-plane strain ε_{33} and t_{33} calculation

An expression for calculating t_{33} sufficiently far from the vertex corners can be obtained in a straightforward manner, if a study of the out-of-plane strain ε_{33} is done, as in [15,16]. Assuming the validity of the Williams series expansion for the out-of-plane component σ_{33} as in Eq. (2), the σ_{ii} stresses in the vicinity of the crack front particularized for the direction $\theta = 0$ are given by

$$\begin{aligned}
\sigma_{11}(r,0) &= \frac{K_{\mathrm{I}}}{\sqrt{2\pi r}} + t_{11} \\
\sigma_{22}(r,0) &= \frac{K_{\mathrm{I}}}{\sqrt{2\pi r}} \\
\sigma_{33}(r,0) &= 2\nu \frac{K_{\mathrm{I}}}{\sqrt{2\pi r}} + t_{33}
\end{aligned} \tag{3}$$

By application of the Hooke's law for an isotropic material, the out-of-plane strain ε_{33} at a given position of the crack front is:

$$\varepsilon_{33} = \frac{1}{E}\left[\sigma_{33} - \nu\left(\sigma_{11} + \sigma_{22}\right)\right] \tag{4}$$

After substitution of (3) in (4), we obtain

$$\varepsilon_{33} = \frac{1}{E}\left[2\nu\frac{K_{\mathrm{I}}}{\sqrt{2\pi r}} + t_{33} - \nu\left(\frac{K_{\mathrm{I}}}{\sqrt{2\pi r}} + t_{11} + \frac{K_{\mathrm{I}}}{\sqrt{2\pi r}}\right)\right] \tag{5}$$

Since $\varepsilon_{33} = \partial u_3/\partial x_3$, the out-of-plane displacement u_3 at the crack front is given by

$$u_3|_{r=0} = \int \varepsilon_{33}|_{r=0}\,\mathrm{d}x_3 \tag{6}$$

and since u_3 must be bounded, ε_{33} cannot include a singular term on r and that is the reason why the singular terms of σ_{11}, σ_{22} and σ_{33} cancel out in Eq. (5). Therefore, the following relationship is obtained:

$$\varepsilon_{33} = \frac{1}{E}\left[t_{33} - \nu t_{11}\right] \tag{7}$$

It can be seen that, at crack front, ε_{33} is dominated by second order terms that cannot be neglected. As a consequence, ε_{33} is, in general, nonzero and strictly speaking, a true plane strain condition with $\varepsilon_{33} = 0$ is not achieved [15].

The latter expression is of practical application, since it enables the computation of t_{33} as:

$$t_{33} = E\varepsilon_{33} + \nu t_{11} \tag{8}$$

The values of ε_{33} and t_{11} have to be known in advance to calculate t_{33}. In this work, they are extracted from the finite element approximation: ε_{33} corresponds directly to the finite element solution at a given position of the crack front, whereas t_{11} is computed using the interaction integral proposed by Nakamura and Parks in [13]. This interaction integral uses the elastic fields associated with a unit line load tangent to the crack front as auxiliary fields.

3 THE T_z OUT-OF-PLANE CONSTRAINT FACTOR APPROACH

The out-of-plane constraint factor T_z was proposed by Guo in [20–22] and its goal is to describe the effect of the out-of-plane constraint on the 3-D stress field. Guo and co-workers assume the following approximation to the stress field under a pure mode I loading:

$$\sigma_{ij}(r,\theta) = \frac{K}{\sqrt{2\pi r}} f_{ij}(\theta) + T\delta_{1i}\delta_{1j} \tag{9}$$

and the constraint factor T_z is defined as

$$T_z = \frac{\sigma_{33}}{\sigma_{11} + \sigma_{22}} \tag{10}$$

Note that T_z is a function of the polar coordinates, $T_z(r,\theta)$, given a normal plane to the crack front. For an isotropic linear elastic body, we have as limiting values $T_z = 0$ for plane stress and $T_z = \nu$ for plane strain conditions [1]. Therefore, the T_z factor provides a measure of the degree of triaxiality of the stress state around the crack front. The f_{ij} terms in Eq. (9) are the trigonometric functions of the Williams series expansion, except $f_{33}(\theta)$ that, to be consistent with the T_z definition, is expressed as

$$f_{33,T_z}(\theta) = T_z(\theta)\left(f_{11}(\theta) + f_{22}(\theta)\right) \tag{11}$$

where the T-stress has been neglected in comparison with the singular terms. For quarter and semi-elliptical cracks, it is shown in [24,25] that the agreement between the numerical results for σ_{33} and the estimation using Eq. (11) is fairly good in the range $0^{\circ} \leq \theta \leq 90^{\circ}$ (approximately), whereas differences are observed in the range $90^{\circ} \leq \theta \leq 180^{\circ}$ at the same radial distance (as

[1] The plane stress and plane strain terms are used here as customary, although they are not strictly applicable to 3-D cracks, see [15,16].

further verified in Section 4). This is the consequence of approximating $T_z(\theta)$ as $T_z(\theta = 0)$ in [24,25]. In these references, it is claimed that the differences in the range $90^o \leq \theta \leq 180^o$ are of little importance because this region has little effect on the crack propagation. In Section 4, it is verified that the consideration of the t_{33}-stress enables a much better agreement in the whole θ-range and enables a proper description of the stress state around a 3-D crack.

In [24], the functional form of T_z as a function of the tangent coordinate x_3 and radial distance r is constructed as a continuous change from a theoretical plane stress on the free surfaces to a theoretical plane strain behavior at points of the crack front sufficiently far from the corner points. Consequently, T_z must satisfy the following boundary conditions on the free surface [22]

$$T_z = 0, \quad \frac{\partial T_z}{\partial x_3} = 0 \tag{12}$$

In addition, the distribution of T_z far from the free boundaries and when $r \to 0$ has a limiting value of ν in isotropic elasticity [24]. Hence, the exact functional form of T_z will be determined by the geometry of the problem considered. The main difficulty of this approach relies on the estimation of T_z, which must be fitted to a numerical solution. As a general analytical expression is still not available, least square methods have been adopted to obtain *ad hoc* coefficients for different T_z distributions which fulfil the boundary and symmetry conditions for a given problem, as is carried out in [24] for the particular case of the quarter-elliptical corner crack. On a given plane normal to the crack front, the T_z distribution in the radial direction for the quarter elliptical corner crack provided in [24] is:

$$T_z = A_1 \left(1 - A_2 \left(\frac{r}{a}\right)^{0.5}\right) \exp\left(-B_1 \left(\frac{r}{a}\right)^{B_2}\right) \tag{13}$$

where a is the minor axis of the quarter-elliptical corner crack, as defined in Fig. 2. According to [24], the coefficient values are given by:

$$\begin{aligned} &A_1 = \nu; \quad A_2 = 0 \\ &B_1 = \frac{B_{11}}{\varphi^{B_{12}}} + \frac{B_{13}}{(90-\varphi)^{B_{14}}} \\ &B_2 = B_{21}\mathrm{exp}\left(\frac{-\varphi}{B_{22}}\right) + B_{23} + \frac{B_{24}}{\varphi}, \end{aligned} \tag{14}$$

where φ defines the position of a point s along the crack front, according to the customary convention for elliptical cracks shown in Fig. 2. The empirical parameters $B_{ij}\,(i = 1, 2; j = 1, 2, 3, 4)$, fitted for $\theta = 0$ and extrapolated for different a/c ratios, with a range of validity defined by $r/a < 1.3$, are [24]:

$$
\begin{aligned}
B_{11} =& 0.48717 + 52.10523\,(a/c) \\
B_{12} =& 0.36432 + 5.96582\,(a/c) - 20.47590\,(a/c)^2 + 31.58187\,(a/c)^3 \\
& - 23.20260\,(a/c)^4 + 6.63021\,(a/c)^5 \\
B_{13} =& 164.24201 - 794.55228\,(a/c) + 2055.33886\,(a/c)^2 \\
& - 2247.54832\,(a/c)^3 + 874.10216\,(a/c)^4 \\
B_{14} =& 1.39811 - 2.88308\,(a/c) + 5.35687\,(a/c)^2 - 4.0019\,(a/c)^3 \\
& + 0.99387\,(a/c)^4 \\
B_{21} =& \exp\left(28.97521 - 33.74222\,(a/c + 0.30026)\right) + 0.46763 \\
B_{22} =& \exp\left(41.78754 - 110.34886\,(a/c + 2.05693)\right) + 4.06779 \\
B_{23} =& -\exp\left(-2.87411 - 0.47004\,(a/c - 1.07951)\right) + 0.60000 \\
B_{24} =& \exp\left(5.83517 - 6.98071\,(a/c + 0.20000)\right) + 0.00496
\end{aligned}
\tag{15}
$$

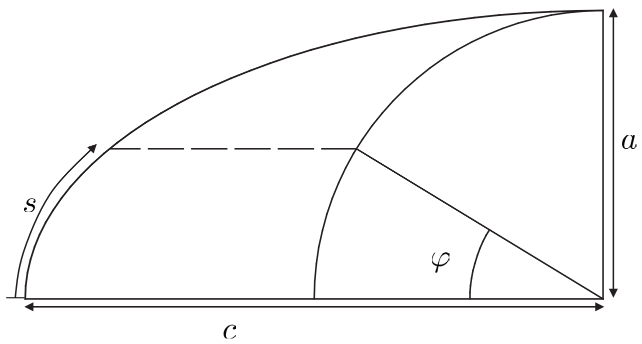

Fig. 2. Angle φ that defines the location of a point s along the elliptical crack front.

In the next section and by means of the reconstruction of σ_{33}, this engineering approach involving T_z will be compared with the use of t_{33}. It will be shown that the introduction of t_{33} enables an accurate description of the out-of-plane stress state.

4 NUMERICAL VERIFICATION

4.1 Geometric and finite element models

The geometric configuration of the corner crack problem coincides with the one studied in [24]. This makes it possible to compare and assess the differences between the consideration of t_{33} and the use of T_z. The crack studied is a quarter-elliptical corner crack embedded in an isotropic elastic plate subjected to uniform tension loading. A sketch of the loads and geometry is given in Fig. 3.

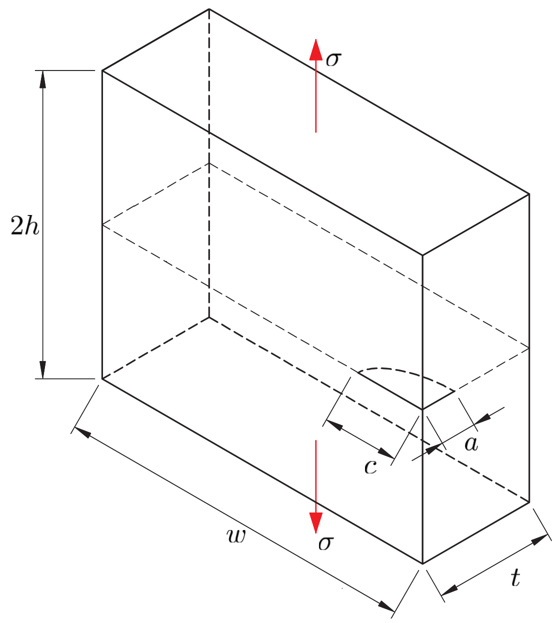

Fig. 3. Sketch of the geometry and loads of the problem.

The elasticity modulus and Poisson's ratio are 200 GPa and 0.3 respectively and the applied stress is $\sigma = 1000$ Pa. Three corner crack geometries with different aspect ratios have been studied: $a/c = 0.2$, $a/c = 0.5$ and $a/c = 1.0$. The plate dimensions relative to the major semi-axis of the quarter-elliptical crack are $w/c = 30$, $t/c = 7.5$, $h/c = 15$ and, therefore, the crack size can be considered small compared to the rest of dimensions. Only half model is analyzed due to the model symmetry with respect to the crack plane.

Finite element meshes with a structured element distribution in the vicinity of crack front have been built. The structured zone is meshed with 20-node hexahedrons around the crack front. Next to the boundaries, the hexahedrons have normal sides to the crack front and crack surface. The rest of the domain is meshed using quadratic tetrahedrons. A general view of one of the meshes can be observed in Fig. 4, the minimum element size being approximately $a/1000$.

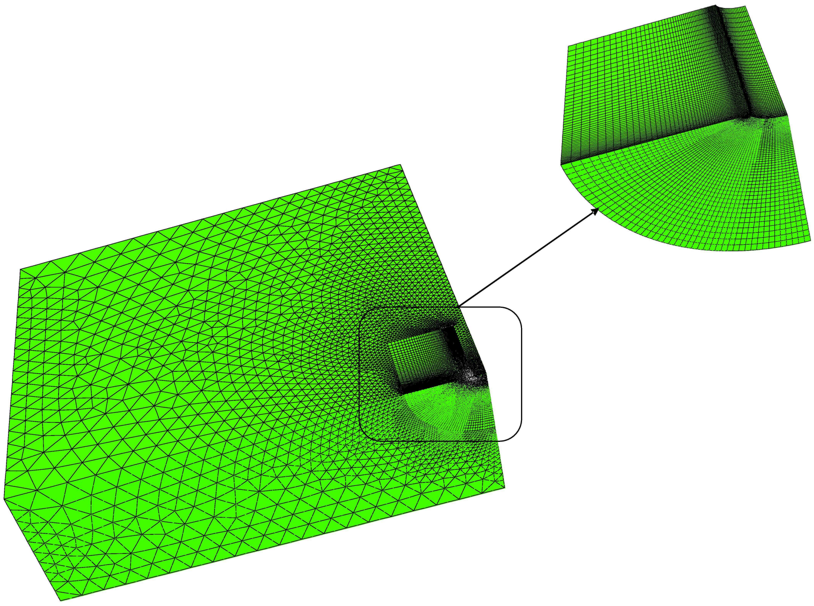

Fig. 4. View of the partially structured mesh with quadratic hexahedrons around crack front.

4.2 K_{I}, t_{11} *and* t_{33} *results*

First of all, the variation of K_{I} and the second order stresses t_{11} and t_{33}

along the crack front has been evaluated. The t_{33}-stress is calculated through Eq. (8), which in turn needs a computation of t_{11} (using the interaction integral proposed in [13]) and an explicit evaluation of ε_{33}. All these magnitudes, conveniently normalized, are plotted in Figs. 5 to 8 for the different a/c ratios. In Fig. 5, a comparison for the SIFs with the approximated solution given by Newman & Raju [32,33] is also provided. The slight differences shown by the results of our study are also reported by other authors presented in Newman & Raju [32] and can be ascribed to the effect of the finite boundaries. Another source of discrepancy between both solutions is their approximate nature (the error of the Newman-Raju solution is less than 5%).

It is interesting to remark that the magnitude of t_{33} is greater than t_{11}, because the contribution of the term $E\varepsilon_{33}$ in Eq. (8) is dominating (note that ε_{33} and t_{33} exhibit a similar trend along the crack front, as can be observed in Figs. 6 and 8). The accuracy of the FE solution near the corner intersections of the crack front with the free boundaries is questionable due to the corner singularity exhibited by ε_{33}. Furthermore, the extraction field used in the interaction integral for the computation of t_{11} assumes a plane strain behavior, a condition that it is not fulfilled in the vicinity of the corner points. Note that mesh distortions due to high curvature impose difficulties to compute smooth solutions for t_{11} using interaction integrals. However, the t_{11} behavior obtained is similar to the one shown by Qu and Wang in [17]. Further details of the behavior of the t_{11} stress terms for semi-elliptical and quarter-elliptical cracks can be found in [17–19].

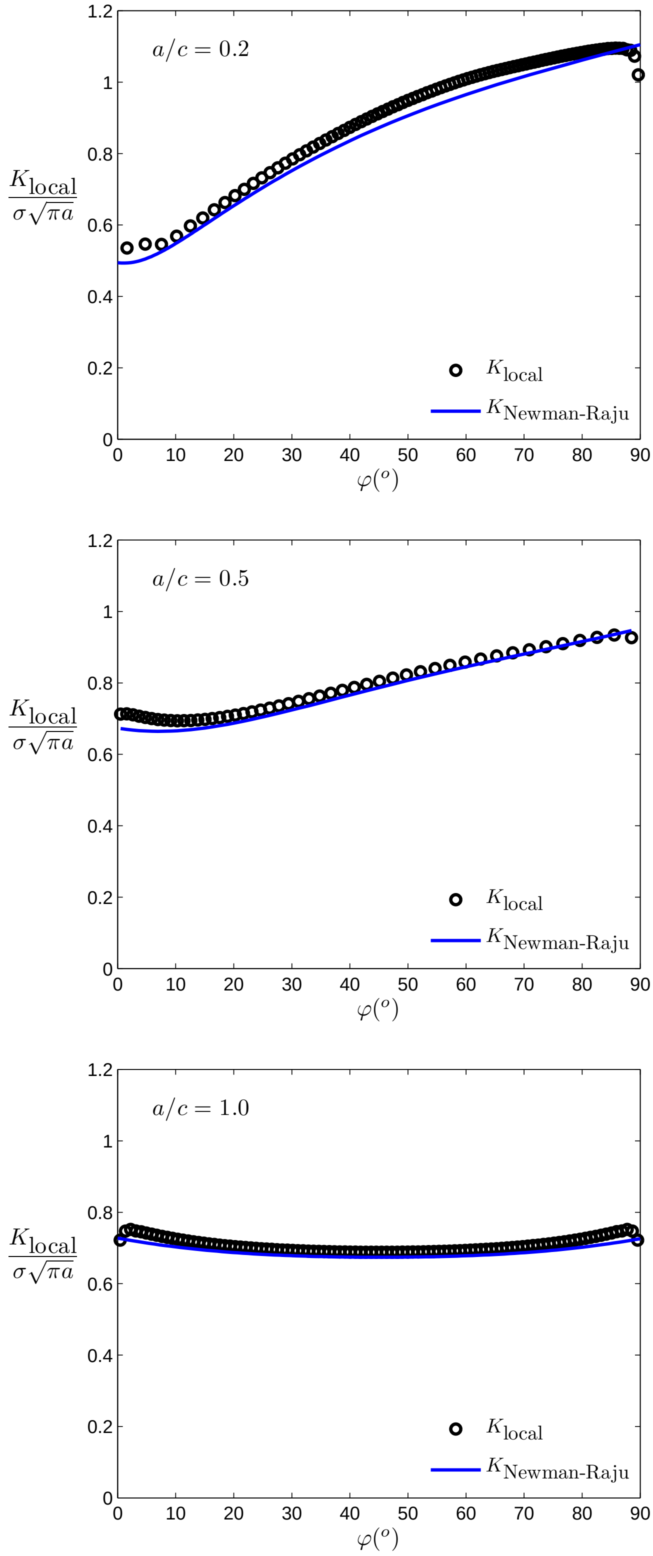

Fig. 5. K_{local} and $K_{\text{Newman-Raju}}$ [32,33]. Normalized variation along crack front for cases $a/c = 0.2$, 0.5 and 1.0.

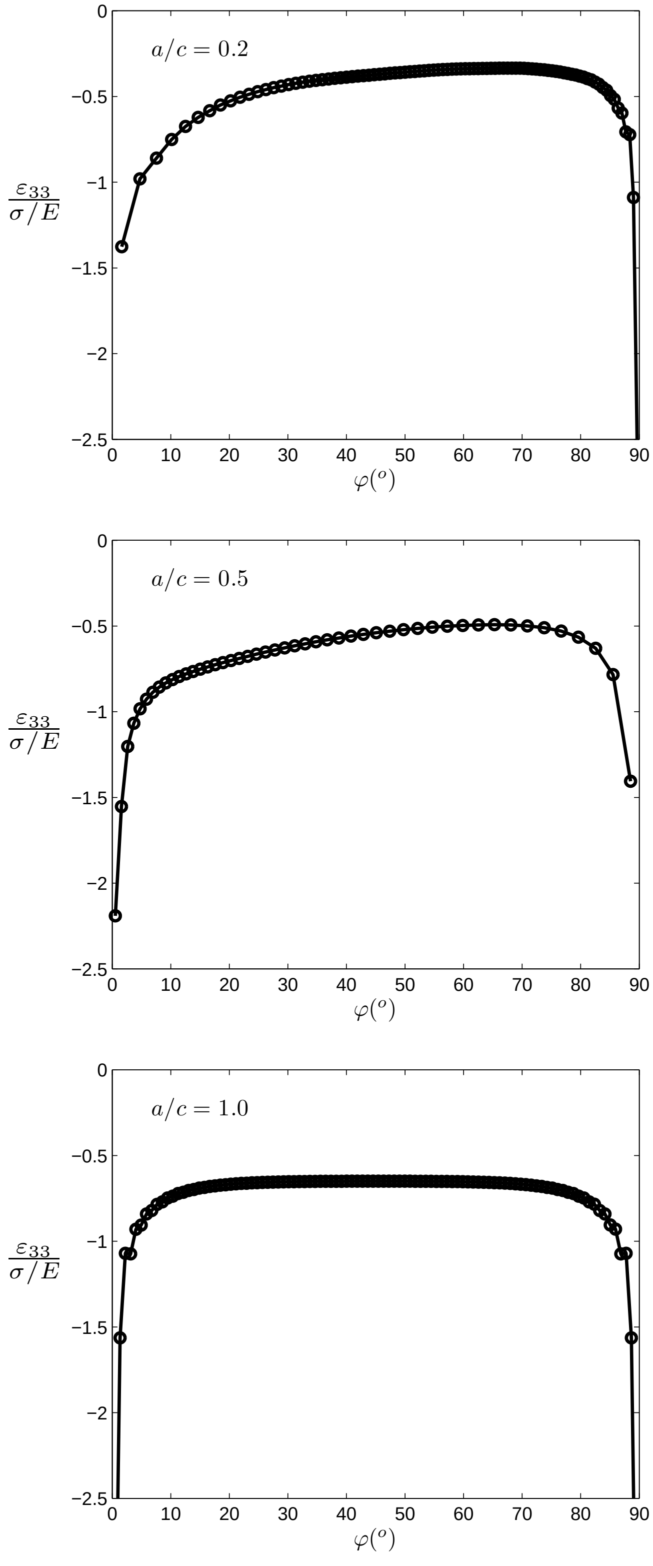

Fig. 6. Normalized variation of ε_{33} along crack front for cases $a/c = 0.2$, 0.5 and 1.0.

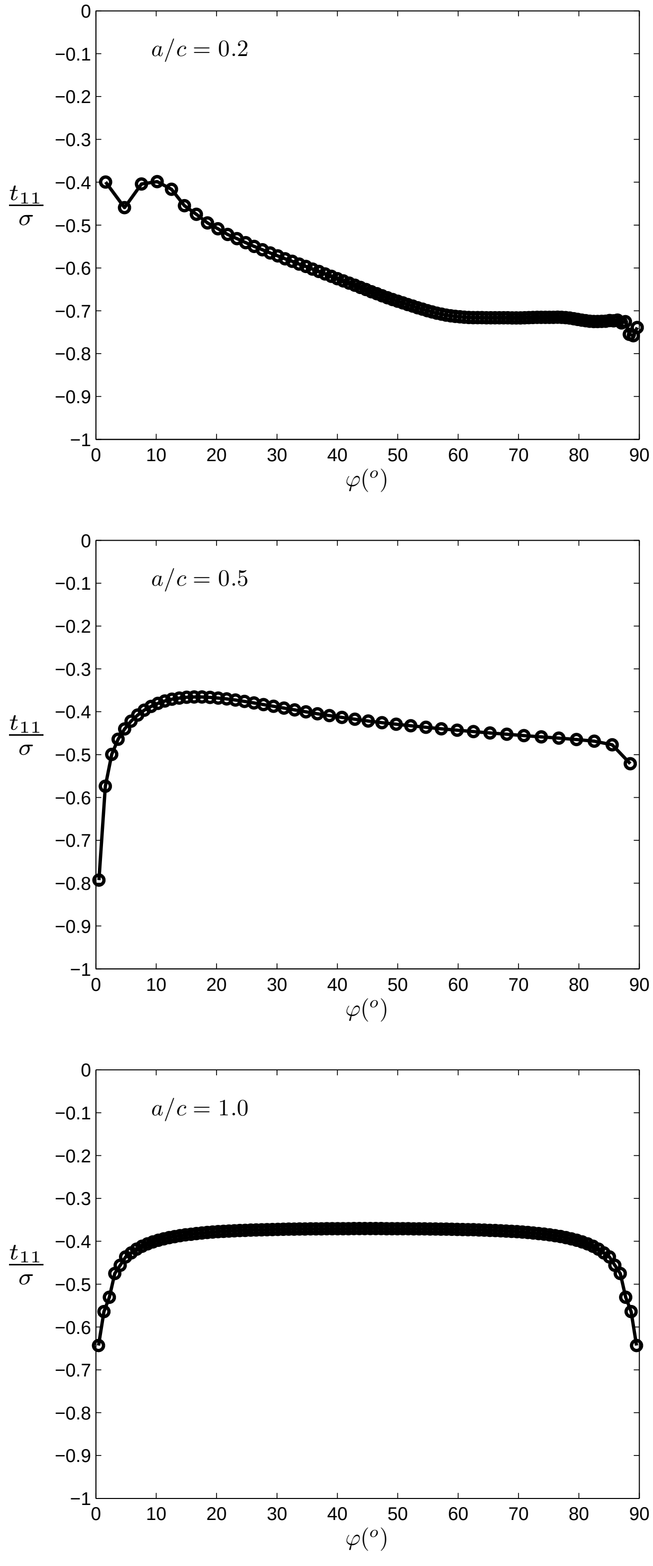

Fig. 7. Normalized variation of T-stress along crack front for cases $a/c = 0.2$, 0.5 and 1.0.

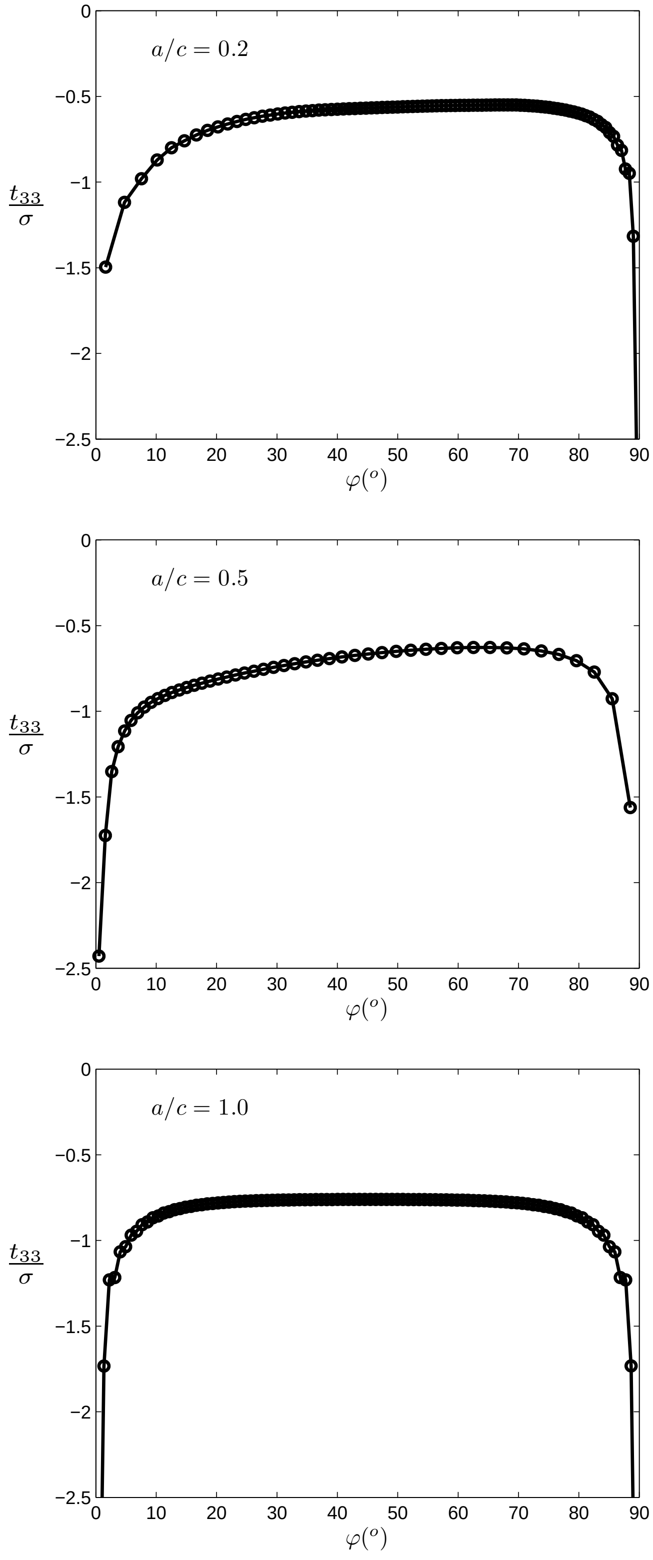

Fig. 8. Normalized variation of t_{33} along crack front for cases $a/c = 0.2$, 0.5 and 1.0.

4.3 Stress state description using T_z and t_{33}

In what follows, a study of the stress state description using T_z and t_{33} is presented. As in [24], the stress state is studied at points located at a very small (but finite) radial distance to the crack front. A small radius circle centered at a given crack front location (see Fig. 9) is used as a path to compare the stress state descriptions given by T_z and t_{33}. The small circle has a radius r and the polar angle θ is varied between 0° and 180°.

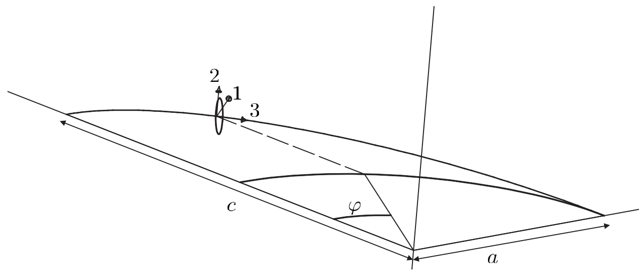

Fig. 9. Circle centered at a crack front location used to study the crack stress state.

The stress components along the circular paths close to the crack front are plotted at five locations defined by the angle φ (see Fig. 2) for each a/c ratio. These locations are approximately[2] $\varphi = 0.9°$, 22.5°, 45°, 67.5° and 88°. Note that the first and last values correspond to locations very close to the free boundaries. The radial distance r/a of the sampled values of stresses along the small circle has been varied for the different aspect ratios a/c to emphasize the generality of the approach.

The plots of results are given in Fig. 10 to Fig. 12 for the aspect ratios $a/c =$ 0.2, 0.5 and 1.0, respectively. Note that the stress components are conveniently normalized by the stress associated with the local stress intensity factor at that

[2] Values of φ are slightly different for each a/c ratio due to the different FE discretizations.

location. The functions $f_{ij}(\theta)$ are the trigonometric functions of the Williams expansion. From Eq. (2), where higher order terms are neglected since the circular path is very close to the crack front, the following relationship must be verified:

$$\frac{\sigma_{ii} - t_{ii}}{K_{\mathrm{I}}/\sqrt{2\pi r}} = f_{ii}(\theta) \tag{16}$$

with

$$\begin{aligned} f_{11}(\theta) &= \cos\frac{\theta}{2}\left(1 - \sin\frac{\theta}{2}\sin\frac{3\theta}{2}\right) \\ f_{22}(\theta) &= \cos\frac{\theta}{2}\left(1 + \sin\frac{\theta}{2}\sin\frac{3\theta}{2}\right) \\ f_{33}(\theta) &= \nu\left(f_{11}(\theta) + f_{22}(\theta)\right) = 2\nu\cos\frac{\theta}{2} \end{aligned} \tag{17}$$

and being $t_{22} = 0$ as commented in Section 1. In Figs. 10 to 12, the function f_{33,T_z} is the expression estimated in [24] using the T_z approach, i.e. $f_{33,T_z} = T_{z(\theta=0)}(f_{11} + f_{22})$ as in Eq. (11). It can be observed that when σ_{33} is reconstructed using the T_z approach, the approximation to σ_{33} is only correct at $\theta = 0°$ (as can be also observed in the analogous figures in [24]). Note that in [24], t_{33} is not taken into account and the coincidence with $f_{33} = \nu(f_{11}+f_{22})$ is not detected for the whole range of θ. Instead, $T_{z(\theta=0)}$ is taken for the generation of $f_{33,T_z} = T_{z(\theta=0)}(f_{11} + f_{22})$, reducing its applicability to the range $\theta = [0°, 90°]$ (approximately) where the deviation from σ_{33} is not so noticeable. This is because the trigonometric functions $(f_{11}+f_{22})$ are zero at $\theta = 180°$ and f_{33,T_z} necessarily deviates from the expected solution when $\theta \neq 0$ because t_{33} is not subtracted. Note that in Figs. 10 to 12, the plots of σ_{33} and $\sigma_{33} - t_{33}$ are shifted a constant magnitude that obviously corresponds to t_{33} at that location.

On the other hand, we observe that the consideration of t_{33} leads to a proper description of the out-of-plane stress for the whole θ range and virtually any location φ along the crack front sufficiently far from the free surfaces. In general, the agreement between $\sigma_{33} - t_{33}$ and $f_{33} = \nu(f_{11} + f_{22})$ is very good at the analyzed locations φ and for the whole range of θ (Figs. 10 to 12). There are only small discrepancies at locations very close to the free surface, where the rapid change in the front curvature affects the quality of the discretization. Other reasons that hinder good estimations in the vicinity of the corner points are that ε_{33} varies very steeply in this zone and that the computation of t_{11} through the interaction integral given in [13] involves a plane strain extraction field. Anyway, it can be observed in Figs. 10 to 12 that this effect is so localized that reasonably good results are obtained at locations very close to the free boundaries, such as $\varphi \approx 0.9°$ and $\varphi \approx 88°$.

As a consequence, the consideration of the t_{33}-stress enables the correct description of the σ_{33} stress and the relationship $f_{33} = \nu(f_{11} + f_{22})$ holds at the crack front for all the locations analyzed. This relationship, although is generally assumed as a plane strain condition, does not necessary imply that $\varepsilon_{33} = 0$, as explained in [15,16]. In fact $\varepsilon_{33} \neq 0$ as clearly shown in Fig. 6. This analysis suggests that a tensor approach that incorporates the second order components t_{ij} [15] instead of the three-parametric approach K-T-T_z can be an alternative for characterizing the 3-D stress state around the crack front. It is also worth remarking that the approach presented here is a good choice to be used in engineering applications, since some approximated expressions are available in the bibliography for the corner crack problem (e.g. SIF values are presented in [32] and t_{ij} in [17]).

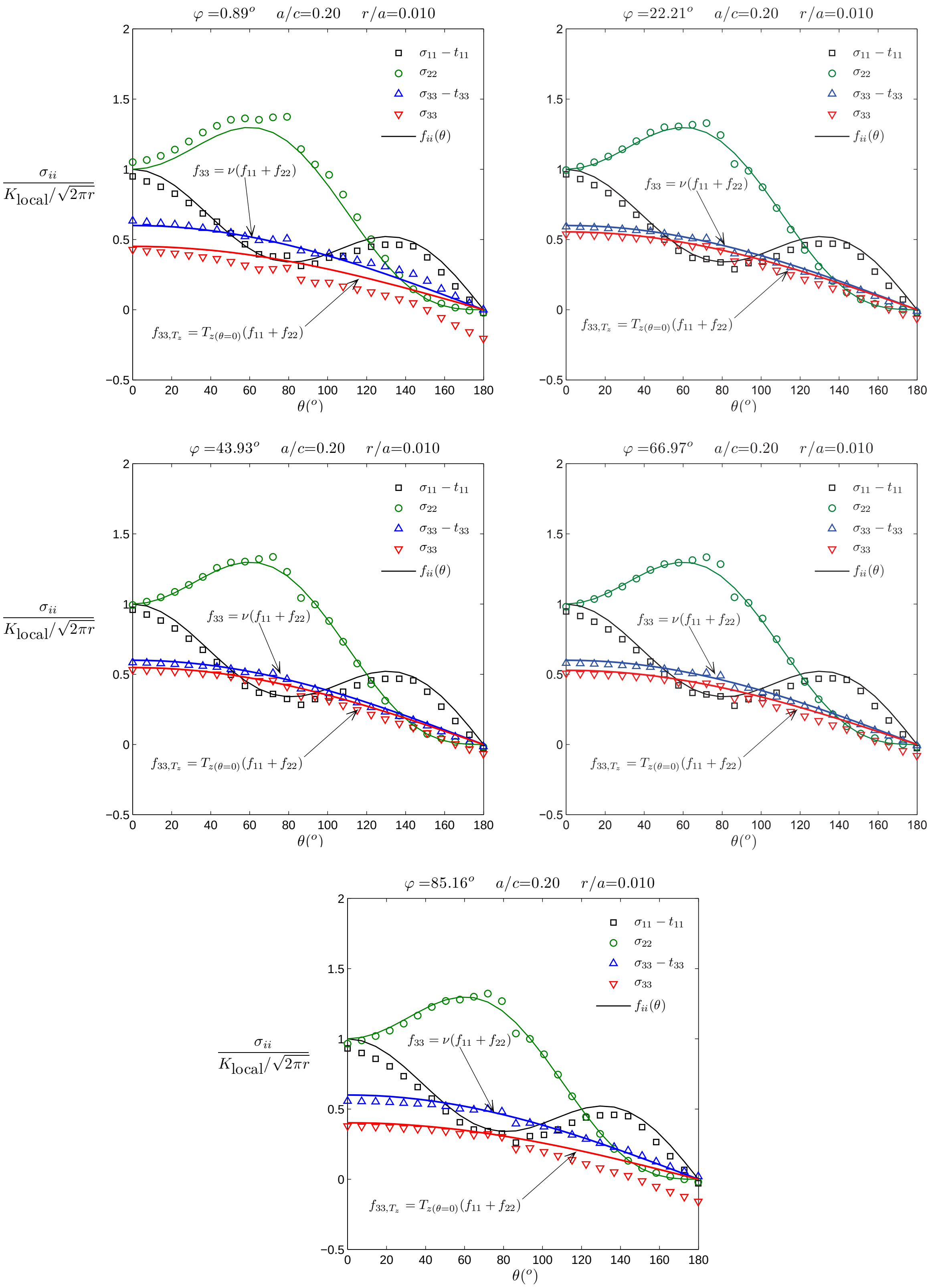

Fig. 10. Stress state along the circular path close to the crack front for five locations φ. Case $a/c = 0.2$ and $r/a = 0.010$.

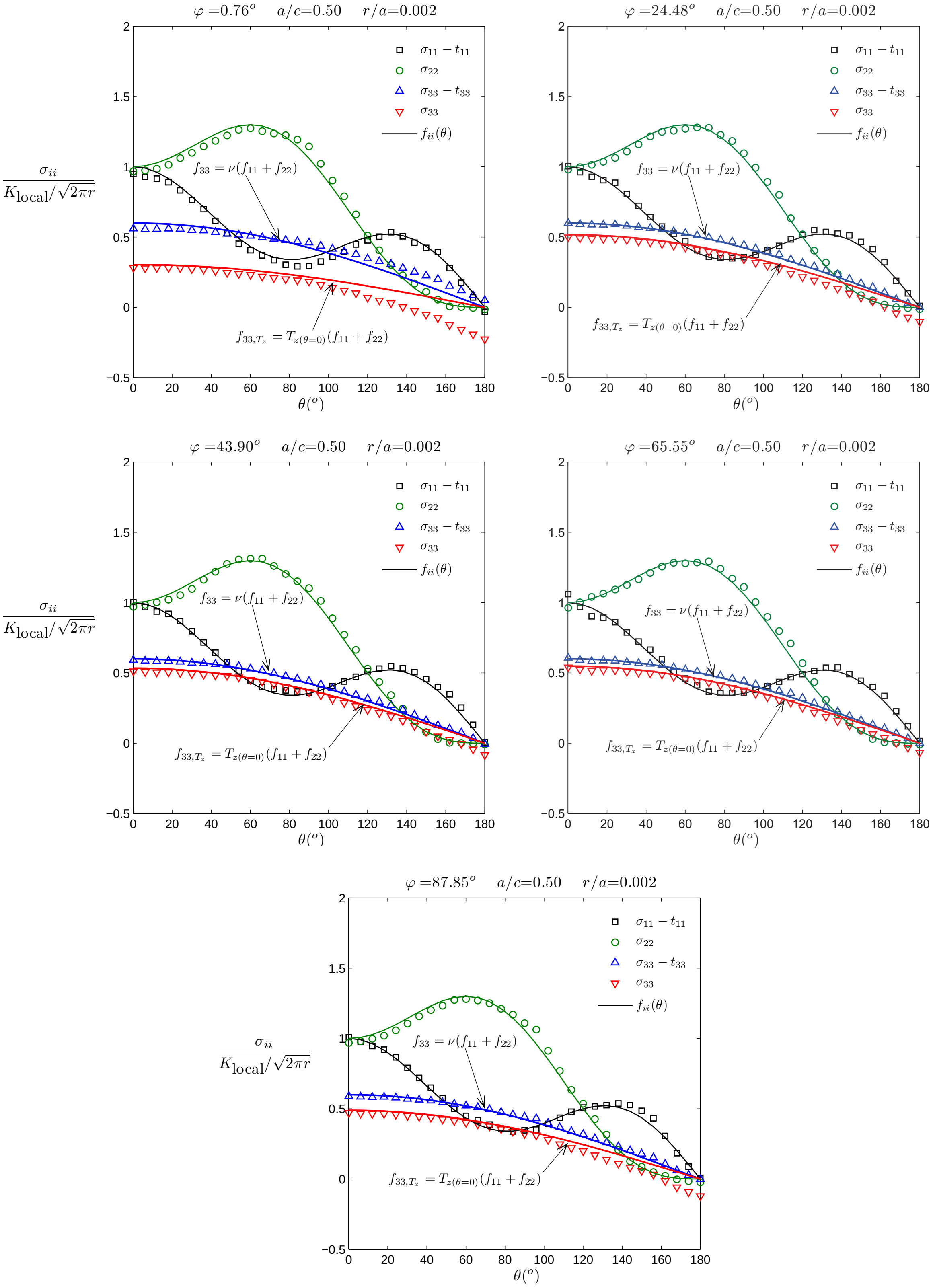

Fig. 11. Stress state along the circular path close to the crack front for five locations φ. Case $a/c = 0.5$ and $r/a = 0.002$.

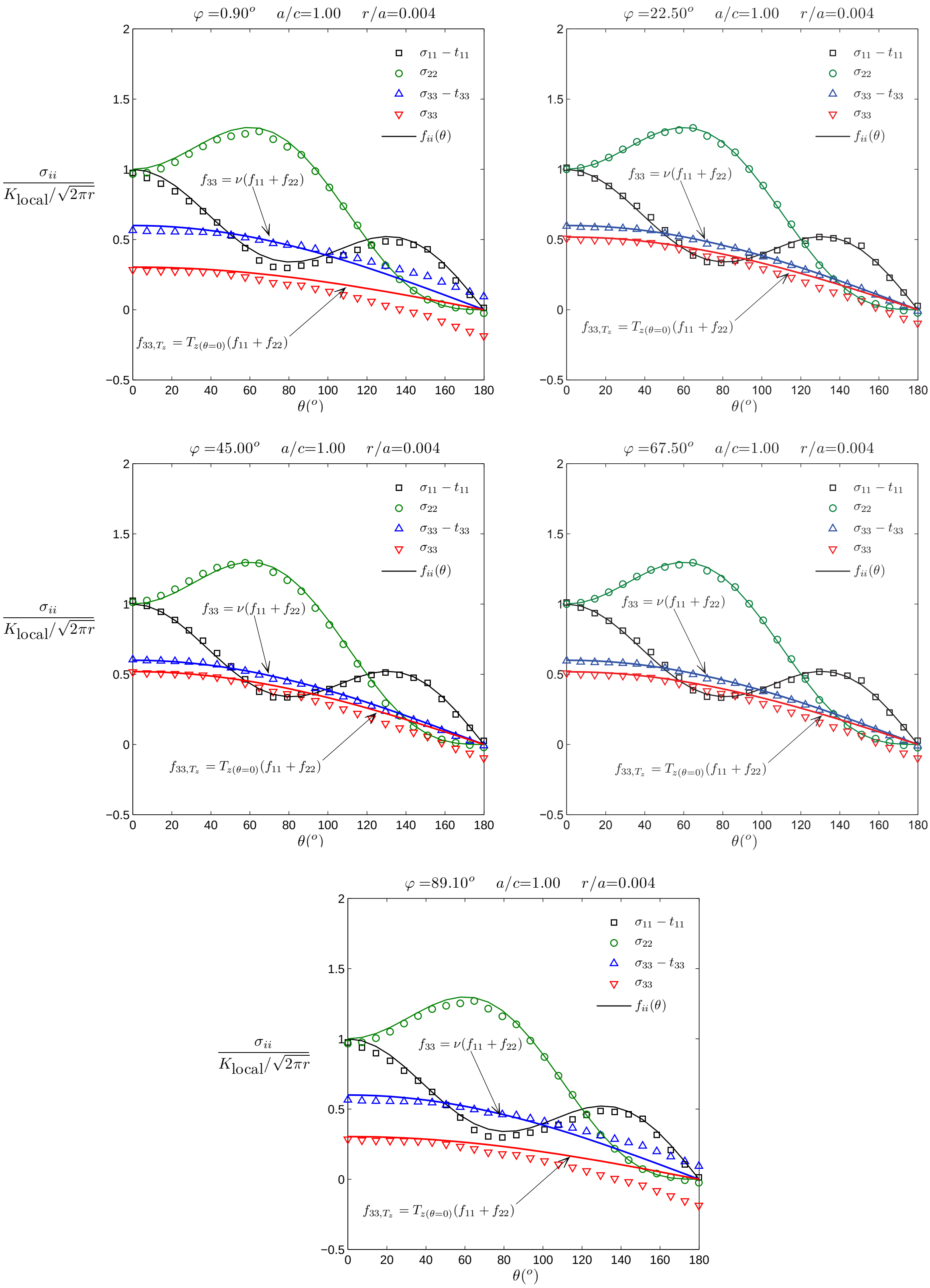

Fig. 12. Stress state along the circular path close to the crack front for five locations φ. Case $a/c = 1.0$ and $r/a = 0.004$.

5 CONCLUSIONS

In this work, an analysis of the description of the out-of-plane constraint around a quarter elliptical crack has been performed. The study compares two approaches for characterizing the constraint: an approach that uses the empirical T_z factor as proposed in [24] and a description based on t_{33} proposed in this work.

The results show that the consideration of the components t_{11} and t_{33} of the t_{ij} tensor is necessary to obtain a correct description of the stress state near the crack front. Instead, the approach that uses K-t_{11}-T_z shows some divergences with respect to the expected values in a wide range of θ. These errors can be ascribed to ignoring the influence of t_{33} and the proper T_z dependence on θ. Therefore, if a factor like T_z is needed, it should take into consideration the t_{33}-stress to provide a more accurate description of the stress state near the crack front. Furthermore, expressions for estimating t_{11} and t_{33} for quarter elliptical cracks are avalaible in [17], which together with the expressions for the SIFs given in e.g. [32], become a natural choice for the characterization of the crack stress state from an engineering point of view.

Acknowledgements

The authors wish to thank the Spanish Ministry of Science and Innovation for the support received in the framework of the project DPI2010-20990 and FI-CYT (Foundation for Scientific and Technological Research, Asturias, Spain), project IB08-171, for partial support of this work.

References

[1] Lin XB, Smith RA. Fatigue shape analysis for corner cracks at fastener holes. Engng Fract Mech 1998;59(1):73–87.

[2] Kim JH, Lee SB, Hong SG. Fatigue crack growth behavior of Al7050-T7451 attachment lugs under flight spectrum variation. Theor Appl Fract Mech 2003;40:135-44.

[3] Mellings SC, Baynham JMW, Adey RA. Advances in crack growth modelling of 3D aircraft structures. In: Bos MJ, editor. Proceedings of the 25th Symposium of the International Committee on Aeronautical Fatigue (ICAF), Rotterdam. Springer Netherlands; 2009, p.789–809.

[4] Lin XB, Smith RA. Finite element modelling of fatigue crack growth of surface cracked plates. Part II: crack shape change. Engng Fract Mech 1999;63:523–40.

[5] Iyyer N, Sarkar S, Merrill R, Phan N. Aircraft life management using crack initiation and crack growth models. P-3C Aircraft experience. Int J Fatigue 2007;29:1584-1607.

[6] Nakamura T, Parks DM. Three-dimensional stress field near the crack front of a thin elastic plate. J Appl Mech 1988;55:805–13.

[7] Guo W. Three dimensional analysis of plastic constraint for through-thickness cracked bodies. Engng Fract Mech 1999;62:383–407.

[8] Kim Y, Zhu XK, Chao YJ. Quantification of constraint on elastic-plastic 3D crack front by the J–A_2 three-term solution. Engng Fract Mech 2001;68:895–914.

[9] Petti JP, Dodd Jr RH. Constraint comparisons for common fracture specimens: C(T)s and SE(B)s. Engng Fract Mech 2004;71:2677–83.

[10] Neimitz A, Galkiewicz J. Fracture Toughness of structural components: influence of constraint. Int J Press Vessels and Pipes 2006;83:42–54.

[11] Shen H, Guo W. 3D constraint effect on 3D fatigue crack propagation. Int J Fatigue 2005;27:617–23.

[12] Williams ML. On the stress distribution at the base of a stationary crack. J Appl Mech 1957;24:109–14.

[13] Nakamura T, Parks DM. Determination of elastic T-stress along three dimensional crack fronts using an interaction integral. Int J Solids Struct 1992;29(13):1597–1611.

[14] Meshii T, Tanaka T. Experimental T_{33}-stress formulation of test specimen thickness effect on fracture toughness in the transition temperature region. Engng Fract Mech 2010;77:867-77.

[15] Giner E, Fernández-Zúñiga D, Fernández-Sáez J, Fernández-Canteli A. A unified analysis of the in-plane and out-of-plane constraints in 3-D LEFM. Int J Mech Sci, submitted.

[16] Giner E, Fernández-Zúñiga D, Fernández-Sáez J, Fernández-Canteli A. On the J_{x_1}-integral and the out-of-plane constraint in a 3D elastic cracked plate loaded in tension. Int J Solids Struct 2010;47(7-8):934–46.

[17] Qu J,Wang X. Solutions of T-stresses for quarter-elliptical corner cracks in finite thickness plates subject to tension and bending. Int J Press Vessels and Pipes 2006;83:593–606.

[18] Wang X, Bell R. Elastic T-stress solutions for semi-elliptical surface cracks in finite thickness plates subject to non-uniform stress distributions. Engng Fract Mech 2004;71:1477–96.

[19] Wang X, Lewis T, Bell R. Estimations of the T-stress for small cracks at notches. Engng Fract Mech 2006;73:366–75.

[20] Guo W. Elasto-plastic three-dimensional crack border field–I. Singular structure of the field. Engng Fract Mech 1993;46:93–104.

[21] Guo W. Elasto-plastic three-dimensional crack border field–II. Asymptotic solution for the field. Engng Fract Mech 1993;46:105–13.

[22] Guo W. Elasto-plastic three-dimensional crack border field–III. Fracture parameters. Engng Fract Mech 1995;51(1):51–71.

[23] She C, Guo W. The out-of-plane constraint of mixed-mode cracks in thin elastic plates. Int J Solids Struct 2007;44:3021–34.

[24] Zhang B, Guo W. Three-dimensional stress state around quarter-elliptical corner cracks in elastic plates subjected to uniform tension loading. Engng Fract Mech 2007;74:386–98.

[25] Zhao J, Guo W, She C. The in-plane and out-of-plane stress constraint factors and $K - T - T_z$ description of a semi-elliptical surface crack. Int J Fatigue 2007;29:435–43.

[26] Hartranft RJ, Sih, GC. The use of eigenfunction expansion in the general solution of three-dimensional crack problems. J Math and Mech 1969;19(2);123–38.

[27] Sih GC. A review of the three dimensional stress problem for a cracked plate. Int J Fract Mech 1971;71(1):39–61.

[28] Benthem JP. State of stress at the vertex of quarter-infinite crack in a half-space. Int J Solids Struct 1977;13:479–92.

[29] Pook LP. Crack profiles and corner point singularities. Fatigue Fract Engng Mater Struct 2000;23:141–50.

[30] Kwon SW, Sun CT. Characteristics of three-dimensional stress fields in plates with a through-the-thickness crack. Int J Fract 2000;104:291–315.

[31] Heyder M, Kolk K, Kuhn G. Numerical and experimental investigations of the influence of corner singularities on 3D fatigue crack propagation. Engng Fract Mech 2005;72:2095–105.

[32] Newman Jr JC, Raju IS. Stress intensity factor equations for cracks in three-dimensional finite bodies. ASTM STP 791; 1983. p. 238–65.

[33] Murakami Y. Stress Intensity Factors Handbook, vol. 2. Oxford, Pergamon Press; 1987. p. 712–15.